HHS Public Access

Author manuscript

*Clin Exp Pharmacol Physiol*. Author manuscript; available in PMC 2024 March 01.

Published in final edited form as:

*Clin Exp Pharmacol Physiol*. 2023 March ; 50(3): 228–237. doi:10.1111/1440-1681.13738.

# Angiotensin receptor blockade with olmesartan alleviates brain pathology in obese OLETF rats

**Carlos J. Rodriguez-Ortiz**[1], **Max A. Thorwald**[2], **Ruben Rodriguez**[2], **Marina Mejias-Ortega**[1,3,4], **Zanett Kieu**[2], **Neilabjo Maitra**[1], **Charlesice Hawkins**[2], **Joanna Valenzuela**[2], **Marcus Peng**[1], **Akira Nishiyama**[5], **Rudy M. Ortiz**[2,*], **Masashi Kitazawa**[1,*]

[1.]Center for Occupational and Environmental Health, Department of Environmental and Occupational Health, Department of Medicine, University of California, Irvine

[2.]Department of Molecular & Cell Biology, University of California, Merced

[3.]Department of Cell Biology, Genetics and Physiology, Instituto de Investigacion Biomedica de Malaga-IBIMA, Facultad de Ciencias, Universidad de Malaga, Spain

[4.]Centro de Investigación Biomedica en Red sobre Enfermedades Neurodegenerativas (CIBERNED), Madrid, Spain

[5.]Department of Pharmacology, Kagawa Medical University, Japan

## Abstract

Metabolic syndrome (MetS) is a rapidly increasing health concern during midlife and is an emerging risk factor for the development of neurodegenerative diseases, such as Alzheimer's disease (AD). While angiotensin receptor blockers (ARB) are widely used for MetS-associated hypertension and kidney disease, its therapeutic potential in the brain during MetS are not well-described. Here, we tested whether treatment with ARB could alleviate the brain pathology and inflammation associated with MetS using the Otsuka Long Evans Tokushima Fatty (OLETF) rat. Here, we report that chronic ARB treatment with olmesartan (10 mg/kg/day by oral gavage for 6 weeks) partially but significantly ameliorated accumulation of oxidized and ubiquitinated proteins, astrogliosis and transformation to neurotoxic astrocytes in the brain of old OLETF rats, which otherwise exhibit the progression of these pathological hallmarks associated with MetS. Additionally, olmesartan treatment restored claudin-5 and ZO-1, markers of the structural integrity of the blood brain barrier as well as synaptic protein PSD-95, which were otherwise decreased in old OLETF rats, particularly in the hippocampus, a critical region in cognition, memory and AD. These data demonstrate that the progression of MetS in OLETF rats is associated with deterioration of various aspects of neuronal integrity that may manifest neurodegenerative conditions and that overactivation of angiotensin receptor directly or indirectly contributes to these

[*]Correspondence to: Masashi Kitazawa, Ph.D., Center for Occupational and Environmental Health, Department of Environmental and Occupational Health, Department of Medicine, University of California, Irvine, Irvine, CA 92617, kitazawa@uci.edu; Rudy M. Ortiz, Ph.D., Department of Molecular & Cell Biology, School of Natural Sciences, University of California, Merced, Merced, CA 95343, rortiz@ucmerced.edu.

CONFLICT OF INTERESTS

None of the authors has any financial or non-financial interests to disclose.

detriments. Thus, olmesartan treatment may slow or delay the onset of degenerative process in the brain and subsequent neurological disorders associated with MetS.

## Graphical Abstract

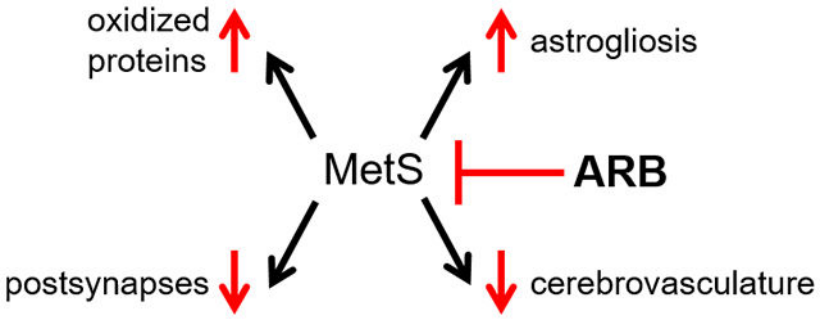


Metabolic syndrome (MetS) favors accumulation of oxidized proteins and astrogliosis and promotes deficits in the integrity of cerebrovasculartureand postsynapses in the brain of OLETF rats. However, ARB treatment ameliorates these toxic consequences induced by MetS.

### Keywords

blood brain barrier; cerebrovasculature; gliosis; hippocampus; neurodegeneration; synapse

## INTRODUCTION

The metabolic syndrome (MetS) is a cluster of metabolic disorders that include hypercholesterolemia, hypertension, obesity, and glucose intolerance with or without insulin resistance among other defects. Among these cluster risk factors, hypercholesterolemia and obesity are strongly correlated to the development of neurodegenerative diseases and associated neural defects, such as Alzheimer's disease (AD) [1]. In addition, obesity dysregulates the renin-angiotensin system (RAS) that leads to hypertension in humans and rodents [2–5]. Angiotensin II (Ang II) mediates its effects by binding its primary receptor type 1 ($AT_1$); however, elevated Ang II or overactivation of $AT_1$ may have deleterious consequences on most organ systems including the heart, kidneys, and brain [6,7]. During pathological conditions, elevated Ang II generates free radicals and oxidative stress, which is mediated by $AT_1$ [8–10]. Similar to its systemic effects, overactivation of $AT_1$ up-regulates reactive oxygen species (ROS) and cerebrovascular oxidative stress in the brain [11,12]. In addition, Ang II induces cerebrovascular injury and inflammation [13,14] by increasing gliosis in the hippocampus [15], a key region for cognitive processing as well as one of the most susceptible brain regions in AD.

Disruption of RAS signaling via angiotensin receptor blockers (ARBs) among others are widely used in patients with hypertension and kidney disease [16,17]. In addition to robustly ameliorating hypertension including the elevated arterial pressure associated with MetS, chronic ARB treatment also reduces systemic oxidative stress and inflammation [18–20]. In stroke-prone spontaneously hypertensive rats (SHRSP), which is characterized by elevated

Ang II [21], chronic ARB treatment (olmesartan x 30 d) reduced oxidative stress in the brain [12]. While the benefits of ARB treatment on brain pathologies has gained considerable attention in recent years [6,7], the effects of the progression of MetS and the potential benefits of ARBs during MetS have not been examined [1].

Here, we investigated the potential benefits of chronic ARB treatment on markers of brain pathologies in a model of MetS, the Otsuka Long-Evans Tokushima Fatty (OLETF) rat, to evaluate the effects of age and MetS on neural injury. OLETF rats are a well-characterized model of MetS that develop defined stages of metabolic defects with age [22–24]. At 16 weeks of age, male OLETF rats present with early onset of insulin resistance and the associated hyperglycemia along with modest progression of other metabolic phenotypes characteristic of the model such as adiposity, dyslipidemia, and hypertension [18,22,23]. By 25 weeks of age, virtually all male OLETF rats develop frank type II diabetes and advanced adiposity and hypertension among other metabolic defects[23,25,26]. Thus, this model allowed us to study potential effects of the manifestation of dysmetabolism and the contribution of AT1 signaling on neural defects with respect to the distinct stage of MetS as defined by the difference in age. The MetS phenotypes including the associated obesity are primarily induced by the hyperphagia caused by a mutation in the *CCKAR* gene, which encodes for the cholecystokinin-1 (CCK-1) receptor [27,28].

## RESULTS

### Younger animals (16 weeks of age)

Because it is well established that aging is a confounding variable in the manifestation of neurological defects including neurodegenerative diseases, we leveraged the use of tissues from younger animals displaying early signs of MetS phenotypes to better assess the timing of the onset of neural pathologies. Thus, some analyses were performed in younger animals initially to gain further insights. Basic metabolic changes are summarized in Table 2[18,22,25,26]. In brief, all presented parameters were elevated in OLETF rats at 16 weeks of age when compared to age-matched control (LETO) rats and ARB treatment normalized the elevated SBP and plasma glucose levels. Our initial brain measurements included quantification of oxidized and ubiquitinated proteins and glial fibrillary acidic protein (GFAP), an astrocyte marker. No discernable differences in any of these variables (Fig. 1A–C) were detected suggesting that at this age and stage of MetS the brain is not susceptible to degeneration and/or defects. Given the lack of robust strain or ARB-associated changes in these variables, no further analyses were performed.

### Older animals (25 weeks of age)

**MetS is associated with accumulation of oxidized and ubiquitinated proteins in the brain and ARB treatment partially ameliorates it.—**Basic metabolic changes of OLETF rats at 25 weeks of age demonstrated advanced adiposity and hypertension and ARB treatment normalized the elevated SBP (Table 2). We examined the brains from these animals to assess the manifestation of neural abnormalities and the potential of chronic ARB treatment to ameliorate these defects. The levels of oxidized and ubiquitinated proteins in whole brain homogenates were measured to assess the degree of potential damage.

Levels of oxidized proteins were increased in OLETF compared to control, while ARB treatment reduced levels (Fig. 2A). Similarly, levels of poly-ubiquitinated proteins were elevated in OLETF compared to control; however, the 31% decrease with ARB treatment was not statistically significant but trended toward partial amelioration ($p = 0.06$; Fig. 2B). To explore whether the autophagy pathway underlies the elevated levels of ubiquitinated proteins in OLETF animals, we analyzed the autophagy markers LC3 and p62. Immunoblot experiments showed no differences in the protein levels of 16 kDa LC3-I, which was predominant in all groups, and 14 kDa LC3-II, a marker for autophagosome activation (Fig. 2C) or p62 (Fig. 2D) among the groups, suggesting that dysregulation of mechanisms others than autophagy mediate the accumulation of ubiquitinated proteins.

**ARB treatment prevents neurotoxic activation of astrocytes in OLETF rats.—** Neuroinflammation was assessed by quantifying glial fibrillary acidic protein (GFAP) and ionized calcium binding adaptor molecule-1 (Iba-1) as markers for astrocytes and microglia, respectively. GFAP protein content was measured by Western blot in the whole brain and by immunostaining particularly in the hippocampus based on earlier study [15] (Fig. 3A and 3B). We were also interested in the hippocampus as it a fundamental region for cognitive processing, specifically learning and memory [29,30], that is particularly sensitive to endogenous and exogenous insults [31,32] and is a critical brain region for AD. In both cases, whole brain and hippocampus GFAP was greater in OLETF compared to control and ARB treatment reduced the levels (Fig. 3A and 3B). Next, the association between increased GFAP immunoreactivity and the increased number of potentially harmful reactive astrocytes expressing complement C3 molecule was assessed. These astrocyte populations exhibited distinct transcriptomic signatures from either homeostatic astrocytes (C3-negative) or displayed neurotoxic phenotypes (C3-positive) [33]. We quantified the ratio of GFAP+:C3- and GFAP+:C3+ astrocytes in the hippocampus and found that the number of C3+ astrocytes were increased in OLETF rats compared to control rats and ARB treatment reduced C3+ astrocytes suggesting that the homeostatic population was restored (Fig. 3C). Similar changes were observed in cortical regions (data not shown). These results indicate that the progression of MetS exacerbates the transformation of astrocytes to highly reactive and neurotoxic astrocytes in the brain via, at least in part, by $AT_1$-mediated effects.

Since C3+ neurotoxic astrocytes are reported to be triggered by activated microglia [33], we attempted to examine characteristics of microglia using several reported markers for homeostatic phenotype (Tmem119) and degenerative phenotype (ferritin) using immunostaining [34,35]. However, we did not detect significant differences in either Tmem119 or ferritin immunoreactivity within Iba1-positive microglia in the brains from these groups (data not shown). More sensitive analysis would be required to definitively determine a shift toward an activated-microglia phenotype in these animals.

**MetS is associated with compromised blood brain barrier.—**To assess the consequences of MetS on the BBB, we measured ZO-1 and claudin-5, the two primary tight junction proteins essential for the maintenance and integrity of cerebrovasculature including the BBB [7,36,37]. Both ZO-1 and claudin-5 were significantly reduced in OLETF rats compared to control (Fig. 4A–4C). While recovery of claudin-5 levels with ARB

treatment were not statistically significant, the changes are indicative of biological trends ($p = 0.08$; Fig. 4C). Thus, at this stage of the MetS, longer duration ARB treatment may be necessary to detect statistically significant changes.

**MetS reduced levels of postsynaptic proteins.—**The reduction of BBB markers and increase of C3+ neurotoxic astrocyte population in OLETF rats indicated that cerebrovascular and/or BBB integrity was impaired or damaged. Thus, we next examined whether loss of synapses was evident in these animals. The density of pre- and postsynaptic markers were quantified in whole brain tissues by immunoblot. Synaptophysin (SYP), postsynaptic density protein 95 (PSD-95), and the AMPA receptor subunit glutamate receptor 2 (GluA2) showed no significant differences among the groups (Fig. 5A–C). On the other hand, the AMPA receptor subunit glutamate receptor 1 (GluA1) was reduced in OLETF compared to control and ARB treatment significantly rescued GluA1 protein levels (Fig. 5D). Next, we quantified SYP and PSD-95 protein levels specifically in the hippocampus since changes in these proteins in this region could be indicative of impaired cognition as previously reported by us [38–40] and others [41–49]. While no differences in hippocampal SYP were detected (Fig. 5E), PSD-95 was lower in OLETF compared to control, but not altered with ARB treatment (Fig. 5F). These results are consistent with the idea that MetS patients are susceptible to impaired cognition, which may manifest initially from postsynaptic deficits.

## DISCUSSION

Metabolic syndrome, such as hypercholesterolemia, hypertension and obesity, is strongly correlated with the risk of neurological disorders and neurodegenerative diseases [1]. However, the contributions of the MetS to the manifestation of neurological disorders have not been examined. Here, we found that the progression of the MetS, which is a function of age, was closely associated with the advancement of neurotoxic astrogliosis and augmented brain and cerebrovascular injury. Important and novel findings of the present study are that: **(1)** advanced onset of the MetS is associated with profound neurological signatures such as increased neurotoxic astrocytes, cerebrovascular damage, and synaptic loss, **(2)** chronic blockade of $AT_1$ ameliorated some of these MetS-associated consequences in the brain, and **(3)** the ARB-associated benefits are likely independent of hypercholesterolemia, hypertension, and obesity (adiposity, described below). These pathological features correlated with deficits in the integrity of vessels in the brain and reduced number of synapsis, while the link between obesity and brain dysfunction, particularly in the hippocampus has been realized [50–52]. However, the complexity of risk factors that constitute the MetS do not likely contribute singularly but in concert to exert deleterious effects including those observed in the present study.

The quantification of some variables of neurological defects in the younger animals was important to demonstrate that the progressive development of MetS in the older animals is associated with the manifestation of neural injury and potentially neurodegeneration. The metabolic disorders that characterize the OLETF rat have been well defined [19,22–26,53–55]; however, a molecular and cellular examination of neurological aspects of this model have not been examined in the progression of MetS. This is important because a recent review of

rodent models of neurodegenerative diseases highlight the lack of MetS models even though a number of models of diabetes, hypercholesterolemia, and obesity exist [1]. The present study also demonstrated that chronic treatment with olmesartan is moderately effective at ameliorating the MetS-associated neural damage. This is consistent with previously reported benefits of olmesartan in the brain [12,37], despite being considered a non-BBB crossing ARB [56]. It is suggested that the orally administered olmesartan acted on $AT_1$ receptors in the circumventricular organ and area postrema, both of which lack a blood–brain barrier and that this may have been sufficient to mediate the direct $AT_1$ effects although this would not discredit the potential for pleiotropic effects [12].

During obesity, elevated Ang II promotes oxidative stress [11], which may lead to brain pathologies including low-grade inflammation [13,15], and disruption to the integrity of the cerebrovasculature [14]. However, these two neuropathological features influence each other promoting the development of a feedback process that exacerbates disease over time. Ang II increases circulating inflammatory cytokines that can disrupt the function of brain vessels [52,57]. Chronic administration of Ang II directly induced cerebrovascular dysfunction, depending, in part, on local activation of $AT_1$, leading to vascular oxidative stress [11]. In SHRSP rats, a similar duration (30 d) treatment of olmesartan at the same dose (10 mg/kg/d) reduced the oxidative stress in the brain when provided either orally or i.c.v. [12]. Additionally, in a mouse model of AD characterized by high levels of ROS, olmesartan decreased oxidative stress in brain vessels and alleviated memory impairments [58] further demonstrating the effectiveness of olmesartan in ameliorating oxidative stress-related neuropathies and substantiates the activation of $AT_1$ contributing to these conditions.

While ARB treatment did not consistently reverse or ameliorate all the neural injuries, it was profoundly effective at completely ameliorating oxidized proteins and neurotoxic astrocytes and tended to improve claudin-5 and ZO-1 suggesting that $AT_1$ activation contributes, at least partially, to these observed neural injuries. In obese and diabetic patients as well as animal models of these conditions, accumulation of oxidized proteins led to dysregulation of the ubiquitin proteasome system (UPS), a fundamental disposal mechanism of misfolded and damaged proteins [59]. Thus, the accumulation of oxidized and ubiquitinated proteins in the brain provides a robust metric of neural damage that appears to be associated with overactivation of $AT_1$.

## Limitations

Because this was an *ex post facto* (retrospective) study in which an unique opportunity to study the potential effects of chronic ARB on ameliorating the strain-associated neural defects, we recognize that a few study limitations require interpretation with caution. Nonetheless, these limitations do not minimize the potential impacts of these results given the paucity of data available in this arena. A recognized limitation is the lack of behavioral data to help confirm the potential translation benefits of the observed improvements with ARB treatment. We also recognize that our experimental design does not identify whether observed rescuing effects by olmesartan is mediated by its blood pressure lowering effect or directly via blockade of $AT_1$ or a combination of both. Further studies that include a group treated with non-RAS targeting antihypertensives such as hydralazine could help addressed

this limitation. Furthermore, the measurement of complement factor 3 (C3), a neural, inflammatory protein that is activated in AD, would have been a valuable contribution to this dataset; however, our efforts to measure protein expression in our samples were unsuccessful and samples were not collected for PCR measurements. Thus, future studies designed specifically to analyze the potential benefits of chronic ARB treatment on markers of neurodegeneration should include behavioral assessments, measurements of C3, and non-RAS targeting antihypertensive drugs to extend the interpretative value of the contribution of $AT_1$ to the progression of neurodegeneration.

In summary, our results demonstrated that the early onset of MetS, which is characterized by hypercholesterolemia, hypertension, and increased adiposity is not associated with profound neural injury; however, advanced stage MetS is associated with astrogliosis, accumulation of toxic protein species, and deficits in the integrity of vessels in the brain and postsynapses. Importantly, chronic blockade of $AT_1$ ameliorated some of the MetS-associated consequences observed in older MetS animals but not in the younger animals suggesting that the persistence of $AT_1$ activation promotes these neural injury and defects. Interestingly, the ARB-associated benefits are likely independent of hypercholesterolemia, hypertension, and obesity (adiposity) individually; however, these MetS risk factors in concert with persistent overactivation of AT1 likely contributed to the manifestation of these neural defects and potentially to neurodegeneration in a more advanced stage of MetS. Thus, chronic treatment of MetS patients with ARBs at an early stage may be critical at helping to prevent or ameliorate the later onset of neural injury and neurodegeneration.

## METHODS

All experimental procedures were reviewed and approved by the institutional animal care and use committees of Kagawa Medical University (Kagawa, Japan) and the University of California, Merced. The analyses described here complement our previous studies designed to enhance our understanding of the contributions of $AT_1$-mediated signaling to the manifestation of MetS and its associated pathologies in multiple tissues. A unique and innovative aspect of the current study is leveraging the opportunity to perform additional and complementary research of the effects of age and the manifestation of MetS on brain pathologies. Thus, brains were used from animals previously described to represent the early stage of insulin resistance and modest MetS phenotype (16 weeks of age, herein referred to as “younger” animals) [18,22] and the advanced MetS phenotype (25 weeks of age, herein referred to as “older” animals) [25,26] but mentioned here briefly for thoroughness.

### Animals

We leveraged the use of brains from animals used in other studies to better investigate the effects of age and the manifestation of the metabolic syndrome. Brains from the younger animals were harvested from animals described in [18,22]. All lean Long–Evans Tokushima Otsuka (LETO; strain control) and obese OLETF rats were obtained from Otsuka Pharmaceutical Co. Ltd. (Tokushima, Japan). Younger animals were 10 week-old males divided into the following groups: **(1)** untreated control + vehicle (0.5% methylcellulose by oral gavage once daily), **(2)** untreated OLETF + vehicle, and **(3)** OLETF + ARB (ARB;

10 mg olmesartan/kg/d by oral gavage x 6 weeks) and were approximately 16 weeks at dissection [18,22]. Older animals were 17 week-old males divided into the same three groups with the exception that older animals were treated with ARB for 8 weeks and were approximately 25 weeks at dissection [25,26]. Olmesartan was selected as the ARB of choice in the primary studies because it is more effective at ameliorating T2D-associated renal injury and hypertension than other ARBs [60] . Because the samples used in this study were derived from rats originally used in independently designed studies, the duration of the ARB treatments was different. Nonetheless, this difference did not affect the overall scope of this study because there were no differences in the pathological outcomes measured between control and OLETF rats at 16 weeks of age.

All animals were maintained in groups of three or four animals per cage in a specific pathogen-free facility under controlled temperature (23°C) and humidity (55%) with a 12:12 hr cycle. All animals were given free access to water and standard laboratory rat chow (MF; Oriental Yeast Corp., Tokyo, Japan). All animal procedures were performed in accordance with National Institutes of Health and University of California guidelines and Use Committee at the University of California, Merced.

## Tissue preparation

Animals were decapitated and the brain was quickly collected. One hemibrain (without olfactory bulb and cerebellum) was frozen in dry ice for immunoblot analysis. Hemibrain lysates were prepared by homogenizing frozen tissue in T-Per extraction buffer (150 mg/mL, Pierce), complemented with protease and phosphatase inhibitors (Thermo Fisher Scientific). Lysates were centrifuged at 20,000 x g for 30 min at 4°C and protein concentration was quantified by the Bradford assay (Bio-Rad Laboratories). The other hemibrain was fixed for 48 h in PBS + 4% paraformaldehyde and then cryoprotected in 30% sucrose for immunofluorescence analysis.

## Immunoblotting

Equal amounts of protein were separated on 4-15% Bis-Tris gel and transferred to PVDF membranes. Membranes were blocked for 1 h in Odyssey blocking solution (Li-cor). After blocking, membranes were incubated overnight with one or two primary antibodies in Odyssey blocking solution + 0.2% tween-20 at 4°C (for a detailed list of the primary antibodies used in this study please refer to Table 1). After washes with TBS + 0.1% tween-20, membranes were incubated for 1 h with the specific secondary antibodies at a dilution of 1:20,000 (IRDye, Li-cor) in Odyssey blocking solution + 0.2% tween-20 + 0.01% SDS. In the case of ZO-1 and claudin-5, the signal was amplified after incubation with primary antibodies with a biotinylated anti-mouse IgG (dilution 1:500; Vector Biolabs, BA-2000) followed by 800CW streptavidin (dilution 1:1000; Li-cor, 926-32230), with both incubations for 1 h in Odyssey blocking solution + 0.2% tween-20 + 0.01% SDS. Blots were scanned in an Odyssey infrared imager (Li-cor). Image Studio software version 5.2 (Li-cor) was used for protein quantification. Protein levels were normalized to GAPDH or tubulin. For oxidized protein analysis, 20 μg of protein were derivatized with 2,4-dinitrophenyl and detected using the oxyblot assay (Millipore) following the manufacturer's instructions.

### Immunofluorescence

Coronal sections (40 μm) were baked and pretreated with sodium citrate, 50 mM (pH 6.0), for 10 min at 95°C. After washes, sections were permeabilized with TBS + 0.1% Triton X-100 for 15 min, washed and blocked with 10% normal serum + 1% BSA in TBS + glycine (0.3M) for 1 h. Sections were incubated overnight with primary antibodies (1:50 dilution) at 4°C. After washes, sections were incubated with the appropriate secondary Alexa Fluor-conjugated antibodies (1:200; Thermo Fisher Scientific) for 2 h, washed, counterstained with DAPI (300nM for 5 min), and mounted with Fluoromount-G (SouthernBiotech). 16-bit grayscale pictures from the dorsal hippocampus were taken under an EVOSfl (AMG) fluorescence microscope using a 40x objective. After background subtraction, minimum and maximum brightness/contrast levels were adjusted to remove unspecific signal (unspecific signal was determined using a section without primary antibody; one per rat per staining). Mean intensity was computed in the CA1 and CA3 regions of the hippocampus (three pictures per region from three to four sections per animal). Analysis was performed using ImageJ software version 1.51j8 (NIH).

### ZO-1 immunofluorescence analysis

14-bit grayscale Z-stack (pitch 0.2μm) pictures from the dorsal hippocampus were taken under a BZ-X700 Keyence fluorescence microscope using a 60x oil-immersion objective. Surface masks were created for collagen and ZO-1 to calculate the volume occupied by ZO-1 within vessels using Imaris (Bitplane Inc.). Five vessels per section were analyzed (three to four sections per animal).

### Statistical analysis

Means (±SEM) were compared among the groups by one-way analysis of variance (ANOVA) followed by Fisher's post-hoc tests if normally distributed (Anderson-Darling test); otherwise, datasets were compared using Kruskal-Wallis test followed by Dunn's post-hoc test. Significance was set at $p$-value ≤0.05 All Analyses were done in Prism 9 software (Graphpad Software LLC, San Diego, CA).

## ACKNOWLEDGEMENTS

This study was funded in part by the National Institutes of Health (NIH) R01-ES024331 to MK and NIH National Heart, Lung, and Blood Institute (NHLBI) R01-HL091767 and a grant from to AstraZeneca to RMO. MAT and RR were supported by NIH National Institute on Minority Health and Health Disparities (NIMHD) T37-MD001480.

## AVAILABILITY OF DATA AND MATERIALS

All data and materials described in this study are available upon reasonable request.

## REFERENCES

1. Bem AF de, Krolow R, Farias HR, Rezende VL de, Gelain DP, Moreira JCF, et al. Animal Models of Metabolic Disorders in the Study of Neurodegenerative Diseases: An Overview. Front Neurosci [Internet]. 2020 Jan 18 [cited 2021 Aug 18];14. Available from: /pmc/articles/PMC7848140/
2. Engeli S, Böhnke J, Gorzelniak K, Janke J, Schling P, Bader M, et al. Weight loss and the renin-angiotensin-aldosterone system. Hypertens (Dallas, Tex 1979). 2005 Mar;45(3):356–62.

3. Furukawa S, Fujita T, Shimabukuro M, Iwaki M, Yamada Y, Nakajima Y, et al. Increased oxidative stress in obesity and its impact on metabolic syndrome. J Clin Invest [Internet]. 2004 [cited 2021 Mar 23];114(12):1752–61. Available from: https://pubmed.ncbi.nlm.nih.gov/15599400/ [PubMed: 15599400]
4. Roberts CK, Barnard RJ, Sindhu RK, Jurczak M, Ehdaie A, Vaziri ND. Oxidative stress and dysregulation of NAD(P)H oxidase and antioxidant enzymes in diet-induced metabolic syndrome. Metabolism. 2006 Jul 1;55(7):928–34. [PubMed: 16784966]
5. Boustany CM, Bharadwaj K, Daugherty A, Brown DR, Randall DC, Cassis LA. Activation of the systemic and adipose renin-angiotensin system in rats with diet-induced obesity and hypertension. Am J Physiol Regul Integr Comp Physiol. 2004 Oct;287(4):R943–9. [PubMed: 15191907]
6. Saavedra JM. Angiotensin II AT1 receptor blockers as treatments for inflammatory brain disorders. Clin Sci (Lond) [Internet]. 2012 Nov [cited 2021 Aug 18];123(10):567. Available from: /pmc/articles/PMC3501743/ [PubMed: 22827472]
7. Unger T Inhibiting angiotensin receptors in the brain: possible therapeutic implications. http://dx.doi.org/101185/030079903125001974 [Internet]. 2008 [cited 2021 Aug 18];19(5):445–8. Available from: https://www.tandfonline.com/doi/abs/10.1185/030079903125001974
8. Touyz RM. Experimental Physiology-Symposium Report Intracellular mechanisms involved in vascular remodelling of resistance arteries in hypertension: role of angiotensin II. Exp Physiol [Internet]. 2005 [cited 2021 Apr 12];90(4):449–55. Available from: https://physoc.onlinelibrary.wiley.com/doi/abs/10.1113/expphysiol.2005.030080 [PubMed: 15890798]
9. Bendall JK, Cave AC, Heymes C, Gall N, Shah AM. Pivotal role of a gp91phox-containing NADPH oxidase in angiotensin II-induced cardiac hypertrophy in mice. Circulation. 2002 Jan 22;105(3):293–6. [PubMed: 11804982]
10. Johar S, Cave AC, Narayanapanicker A, Grieve DJ, Shah AM. Aldosterone mediates angiotensin II-induced interstitial cardiac fibrosis via a Nox2-containing NADPH oxidase. FASEB J • FJ Express Full-Length Artic [Internet]. 2006 Jul [cited 2021 Apr 12];20(9):1546–8. Available from: https://faseb.onlinelibrary.wiley.com/doi/abs/10.1096/fj.05-4642fje
11. Capone C, Faraco G, Peterson JR, Coleman C, Anrather J, Milner TA, et al. Central cardiovascular circuits contribute to the neurovascular dysfunction in angiotensin II hypertension. J Neurosci [Internet]. 2012 Apr 4 [cited 2021 Apr 28];32(14):4878–86. Available from: https://www.jneurosci.org/content/32/14/4878 [PubMed: 22492044]
12. Araki S, Hirooka Y, Kishi T, Yasukawa K, Utsumi H, Sunagawa K. Olmesartan reduces oxidative stress in the brain of stroke-prone spontaneously hypertensive rats assessed by an in vivo ESR method. Hypertens Res 2009 3212 [Internet]. 2009 Sep 18 [cited 2021 Aug 18];32(12):1091–6. Available from: https://www.nature.com/articles/hr2009160
13. Marvar PJ, Thabet SR, Guzik TJ, Lob HE, McCann LA, Weyand C, et al. Central and peripheral mechanisms of T-lymphocyte activation and vascular inflammation produced by angiotensin II-induced hypertension. Circ Res. 2010 Jul;107(2):263–70. [PubMed: 20558826]
14. Faraco G, Sugiyama Y, Lane D, Garcia-Bonilla L, Chang H, Santisteban MM, et al. Perivascular macrophages mediate the neurovascular and cognitive dysfunction associated with hypertension. J Clin Invest. 2016 Dec;126(12):4674–89. [PubMed: 27841763]
15. Iulita MF, Vallerand D, Beauvillier M, Haupert N, A. Ulysse C, Gagné A, et al. Differential effect of angiotensin II and blood pressure on hippocampal inflammation in mice. J Neuroinflammation [Internet]. 2018 Feb 28 [cited 2021 May 7];15(1):1–14. Available from: 10.1186/s12974-018-1090-z [PubMed: 29301548]
16. Brenner BM, Cooper ME, de Zeeuw D, Keane WF, Mitch WE, Parving H-H, et al. Effects of Losartan on Renal and Cardiovascular Outcomes in Patients with Type 2 Diabetes and Nephropathy. N Engl J Med. 2001 Sep 20;345(12):861–9. [PubMed: 11565518]
17. Lewis EJ, Hunsicker LG, Clarke WR, Berl T, Pohl MA, Lewis JB, et al. Renoprotective Effect of the Angiotensin-Receptor Antagonist Irbesartan in Patients with Nephropathy Due to Type 2 Diabetes. N Engl J Med. 2001 Sep 20;345(12):851–60. [PubMed: 11565517]
18. Rodriguez R, Escobedo B, Lee AY, Thorwald M, Godoy-Lugo JA, Nakano D, et al. Simultaneous angiotensin receptor blockade and glucagon-like peptide-1 receptor activation ameliorate albuminuria in obese insulin-resistant rats. Clin Exp Pharmacol Physiol [Internet].

2020 Mar 1 [cited 2021 Mar 23];47(3):422–31. Available from: https://pubmed.ncbi.nlm.nih.gov/31675433/ [PubMed: 31675433]

19. Minas JN, Thorwald MA, Conte D, Vázquez-Medina JP, Nishiyama A, Ortiz RM. Angiotensin and mineralocorticoid receptor antagonism attenuates cardiac oxidative stress in angiotensin II-infused rats. Clin Exp Pharmacol Physiol [Internet]. 2015 Nov 1 [cited 2021 Mar 23];42(11):1178–88. Available from: https://pubmed.ncbi.nlm.nih.gov/26234762/ [PubMed: 26234762]
20. Lara LS, McCormack M, Semprum-Prieto LC, Shenouda S, Majid DSA, Kobori H, et al. AT 1 receptor-mediated augmentation of angiotensinogen, oxidative stress, and inflammation in ANG II-salt hypertension. Am J Physiol Physiol [Internet]. 2012 Jan 1 [cited 2021 Mar 23];302(1):F85–94. Available from: https://www.physiology.org/doi/10.1152/ajprenal.00351.2011
21. Castro-Moreno, Pardo J, Hernández-Muñoz R, López-Guerrero J, Del Valle-Mondragón L, Pastelín-Hernández G, et al. Captopril avoids hypertension, the increase in plasma angiotensin II but increases angiotensin 1-7 and angiotensin II-induced perfusion pressure in isolated kidney in SHR. Auton Autacoid Pharmacol [Internet]. 2012 Oct [cited 2021 Aug 18];32(3 Pt 4):61–9. Available from: https://pubmed.ncbi.nlm.nih.gov/22994939/ [PubMed: 22994939]
22. Rodriguez R, Minas JN, Vazquez-Medina JP, Nakano D, Parkes DG, Nishiyama A, et al. Chronic AT1 blockade improves glucose homeostasis in obese OLETF rats. J Endocrinol. 2018 Jun;237(3):271–84. [PubMed: 29643115]
23. Kawano K, Hirashima T, Mori S, Saitoh Y, Kurosumi M, Natori T. Spontaneous Long-Term Hyperglycemic Rat With Diabetic Complications: Otsuka Long-Evans Tokushima Fatty (OLETF) Strain. Diabetes [Internet]. 1992 Nov 1 [cited 2021 Aug 18];41(11):1422–8. Available from: https://diabetes.diabetesjournals.org/content/41/11/1422 [PubMed: 1397718]
24. Rodriguez R, Viscarra J, Minas J, Nakano D, Nishiyama A, Ortiz R. Angiotensin receptor blockade increases pancreatic insulin secretion and decreases glucose intolerance during glucose supplementation in a model of metabolic syndrome. Endocrinology [Internet]. 2012 Apr [cited 2021 Aug 18];153(4):1684–95. Available from: https://pubmed.ncbi.nlm.nih.gov/22355070/ [PubMed: 22355070]
25. Godoy-Lugo JA, Thorwald MA, Hui DY, Nishiyama A, Nakano D, Soñanez-Organis JG, et al. Chronic angiotensin receptor activation promotes hepatic triacylglycerol accumulation during an acute glucose challenge in obese-insulin-resistant OLETF rats. Endocr 2021 [Internet]. 2021 Jul 29 [cited 2021 Aug 18];1–16. Available from: https://link.springer.com/article/10.1007/s12020-021-02834-7
26. Thorwald MA, Godoy-Lugo JA, Rodriguez GJ, Rodriguez MA, Jamal M, Kinoshita H, et al. Nrf2-related gene expression is impaired during a glucose challenge in type II diabetic rat hearts. Free Radic Biol Med. 2019 Jan 1;130:306–17. [PubMed: 30316779]
27. Moran TH. Unraveling the Obesity of OLETF Rats. Physiol Behav [Internet]. 2008 Apr 22 [cited 2022 Jan 5];94(1):71. Available from: /pmc/articles/PMC2399903/ [PubMed: 18190934]
28. Miyasaka K, Kanai S, Ohta M, Kawanami T, Kono A, Funakoshi A. Lack of satiety effect of cholecystokinin (CCK) in a new rat model not expressing the CCK-A receptor gene. Neurosci Lett. 1994 Oct 24;180(2):143–6. [PubMed: 7700567]
29. Burgess N, Maguire EA, O'Keefe J. The human hippocampus and spatial and episodic memory. Neuron [Internet]. 2002 Aug 15 [cited 2021 Jul 27];35(4):625–41. Available from: https://pubmed.ncbi.nlm.nih.gov/12194864/ [PubMed: 12194864]
30. Moser M, Moser E. Functional differentiation in the hippocampus. Hippocampus [Internet]. 1998 [cited 2021 Jul 27];8(6):608–19. Available from: https://pubmed.ncbi.nlm.nih.gov/9882018/ [PubMed: 9882018]
31. Stoltenburg-Didinger G Neuropathology of the hippocampus and its susceptibility to neurotoxic insult. Neurotoxicology. 1994;15(3):445–50. [PubMed: 7854577]
32. Walsh TJ, Emerich DF. The hippocampus as a common target of neurotoxic agents. Toxicology. 1988 Apr 1;49(1):137–40. [PubMed: 3287689]
33. Liddelow SA, Guttenplan KA, Clarke LE, Bennett FC, Bohlen CJ, Schirmer L, et al. Neurotoxic reactive astrocytes are induced by activated microglia. Nat 2017 5417638 [Internet]. 2017 Jan 18 [cited 2021 Nov 2];541(7638):481–7. Available from: https://www.nature.com/articles/nature21029

34. Mehlhase J, Gieche J, Widmer R, Grune T. Ferritin levels in microglia depend upon activation: Modulation by reactive oxygen species. Biochim Biophys Acta - Mol Cell Res. 2006 Aug 1;1763(8):854–9.
35. Kenkhuis B, Somarakis A, de Haan L, Dzyubachyk O, IJsselsteijn ME, de Miranda NFCC, et al. Iron loading is a prominent feature of activated microglia in Alzheimer's disease patients. Acta Neuropathol Commun 2021 91 [Internet]. 2021 Feb 17 [cited 2021 Nov 2];9(1):1–15. Available from: https://actaneurocomms.biomedcentral.com/articles/10.1186/s40478-021-01126-5
36. Lochhead JJ, Yang J, Ronaldson PT, Davis TP. Structure, Function, and Regulation of the Blood-Brain Barrier Tight Junction in Central Nervous System Disorders. Front Physiol. 2020 Aug 6;0:914.
37. Pelisch N, Hosomi N, Mori H, Masaki T, Nishiyama A. RAS inhibition attenuates cognitive impairment by reducing blood- brain barrier permeability in hypertensive subjects. Curr Hypertens Rev [Internet]. 2013 Jul 5 [cited 2021 Aug 18];9(2):93–8. Available from: https://pubmed.ncbi.nlm.nih.gov/23971690/ [PubMed: 23971690]
38. Medeiros R, Kitazawa M, Passos G, Baglietto-Vargas D, Cheng D, Cribbs D, et al. Aspirin-triggered lipoxin A4 stimulates alternative activation of microglia and reduces Alzheimer disease-like pathology in mice. Am J Pathol [Internet]. 2013 May [cited 2021 Nov 2];182(5):1780–9. Available from: https://pubmed.ncbi.nlm.nih.gov/23506847/ [PubMed: 23506847]
39. Blurton-Jones M, Kitazawa K, Martinez-Coria H, Castello N, Müller F, Loring J, et al. Neural stem cells improve cognition via BDNF in a transgenic model of Alzheimer disease. Proc Natl Acad Sci U S A [Internet]. 2009 Aug 11 [cited 2021 Nov 2];106(32):13594–9. Available from: https://pubmed.ncbi.nlm.nih.gov/19633196/ [PubMed: 19633196]
40. Yamasaki TR, Blurton-Jones M, Morrissette DA, Kitazawa M, Oddo S, LaFerla FM. Neural Stem Cells Improve Memory in an Inducible Mouse Model of Neuronal Loss. J Neurosci [Internet]. 2007 Oct 31 [cited 2021 Nov 2];27(44):11925. Available from: /pmc/articles/PMC6673368/ [PubMed: 17978032]
41. Wang S, Yu L, Yang H, Li C, Hui Z, Xu Y, et al. Oridonin Attenuates Synaptic Loss and Cognitive Deficits in an Aβ1–42-Induced Mouse Model of Alzheimer's Disease. PLoS One [Internet]. 2016 Mar 1 [cited 2021 Nov 2];11(3):e0151397. Available from: https://journals.plos.org/plosone/article?id=10.1371/journal.pone.0151397 [PubMed: 26974541]
42. Cui S, Yang M, Zhang Y, Zheng V, Zhang H, Gurney M, et al. Protection from Amyloid β Peptide-Induced Memory, Biochemical, and Morphological Deficits by a Phosphodiesterase-4D Allosteric Inhibitor. J Pharmacol Exp Ther [Internet]. 2019 [cited 2021 Nov 2];371(2):250–9. Available from: https://pubmed.ncbi.nlm.nih.gov/31488603/ [PubMed: 31488603]
43. Migaud M, Charlesworth P, Dempster M, Webster L, Watabe A, Makhinson M, et al. Enhanced long-term potentiation and impaired learning in mice with mutant postsynaptic density-95 protein. Nature [Internet]. 1998 Dec 3 [cited 2021 Nov 2];396(6710):433–9. Available from: https://pubmed.ncbi.nlm.nih.gov/9853749/
44. Pollak D, Herkner K, Hoeger H, Lubec G. Behavioral testing upregulates pCaMKII, BDNF, PSD-95 and egr-1 in hippocampus of FVB/N mice. Behav Brain Res [Internet]. 2005 Aug 30 [cited 2021 Nov 2];163(1):128–35. Available from: https://pubmed.ncbi.nlm.nih.gov/15927279/ [PubMed: 15927279]
45. Moyano S, Del Río J, Frechilla D. Acute and chronic effects of MDMA on molecular mechanisms implicated in memory formation in rat hippocampus: surface expression of CaMKII and NMDA receptor subunits. Pharmacol Biochem Behav [Internet]. 2005 Sep [cited 2021 Nov 2];82(1):190–9. Available from: https://pubmed.ncbi.nlm.nih.gov/16154187/ [PubMed: 16154187]
46. Yang S, Liu C, Chung M, Huang H, Yeh G, Wong C, et al. Alterations of postsynaptic density proteins in the hippocampus of rat offspring from the morphine-addicted mother: Beneficial effect of dextromethorphan. Hippocampus [Internet]. 2006 [cited 2021 Nov 2];16(6):521–30. Available from: https://pubmed.ncbi.nlm.nih.gov/16598705/ [PubMed: 16598705]
47. Le Grevès M, Zhou Q, Berg M, Le Grevès P, Fhölenhag K, Meyerson B, et al. Growth hormone replacement in hypophysectomized rats affects spatial performance and hippocampal levels of NMDA receptor subunit and PSD-95 gene transcript levels. Exp brain Res [Internet]. 2006 Aug [cited 2021 Nov 2];173(2):267–73. Available from: https://pubmed.ncbi.nlm.nih.gov/16633806/ [PubMed: 16633806]

48. Chen W, Chang H, Wong C, Huang L, Yang C, Yang S. Impaired expression of postsynaptic density proteins in the hippocampal CA1 region of rats following perinatal hypoxia. Exp Neurol [Internet]. 2007 Mar [cited 2021 Nov 2];204(1):400–10. Available from: https://pubmed.ncbi.nlm.nih.gov/17270176/ [PubMed: 17270176]
49. Nyffeler M, Zhang W, Feldon J, Knuesel I. Differential expression of PSD proteins in age-related spatial learning impairments. Neurobiol Aging [Internet]. 2007 Jan [cited 2021 Nov 2];28(1):143–55. Available from: https://pubmed.ncbi.nlm.nih.gov/16386336/ [PubMed: 16386336]
50. Morrison CD, Pistell PJ, Ingram DK, Johnson WD, Liu Y, Fernandez-Kim SO, et al. High fat diet increases hippocampal oxidative stress and cognitive impairment in aged mice: Implications for decreased Nrf2 signaling. J Neurochem. 2010;114(6):1581–9. [PubMed: 20557430]
51. Biessels GJ, Reagan LP. Hippocampal insulin resistance and cognitive dysfunction. Nat Rev Neurosci 2015 1611 [Internet]. 2015 Oct 14 [cited 2021 Jul 27];16(11):660–71. Available from: https://www.nature.com/articles/nrn4019
52. Tucsek Z, Toth P, Sosnowska D, Gautam T, Koller A, Sonntag W, et al. Obesity in aging exacerbates blood brain barrier disruption, neuroinflammation and oxidative stress in the mouse hippocampus: effects on expression of genes involved in beta-amyloid generation and Alzheimer's disease (665.1). FASEB J [Internet]. 2014 Apr [cited 2021 Jul 27];28(S1):665.1. Available from: https://faseb.onlinelibrary.wiley.com/doi/full/10.1096/fasebj.28.1_supplement.665.1
53. Rodriguez R, Moreno M, Lee A, Godoy- J, Nakano D, Nishiyama A, et al. Simultaneous GLP-1 receptor activation and angiotensin receptor blockade increase natriuresis independent of altered arterial pressure in obese OLETF rats. Hypertens Res [Internet]. 2018 Oct 1 [cited 2021 Aug 18];41(10):798–808. Available from: https://pubmed.ncbi.nlm.nih.gov/29985448/ [PubMed: 29985448]
54. Rodriguez R, Lee A, Mathis K, Broome H, Thorwald M, Martinez B, et al. Angiotensin receptor and tumor necrosis factor-α activation contributes to glucose intolerance independent of systolic blood pressure in obese rats. Am J Physiol Renal Physiol [Internet]. 2018 [cited 2021 Aug 18];315(4):F1081–90. Available from: https://pubmed.ncbi.nlm.nih.gov/29993275/ [PubMed: 29993275]
55. Abbondante S, Baglietto-Vargas D, Rodriguez-Ortiz CJ, Estrada-Hernandez T, Medeiros R, LaFerla FM. Genetic ablation of tau mitigates cognitive impairment induced by type 1 diabetes. Am J Pathol. 2014;184(3). [PubMed: 24183847]
56. Ho JK, Nation DA. Memory is preserved in older adults taking AT1 receptor blockers. Alzheimer's Res Ther 2017 91 [Internet]. 2017 Apr 26 [cited 2021 Aug 19];9(1):1–14. Available from: https://alzres.biomedcentral.com/articles/10.1186/s13195-017-0255-9
57. Zhang M, Mao Y, Ramirez SH, Tuma RF, Chabrashvili T. Angiotensin II induced cerebral microvascular inflammation and increased blood–brain barrier permeability via oxidative stress. Neuroscience. 2010 Dec 15;171(3):852–8. [PubMed: 20870012]
58. Takeda S, Sato N, Takeuchi D, Kurinami H, Shinohara M, Niisato K, et al. Angiotensin receptor blocker prevented β-amyloid-induced cognitive impairment associated with recovery of neurovascular coupling. Hypertension [Internet]. 2009 Dec [cited 2021 Apr 12];54(6):1345–52. Available from: https://pubmed.ncbi.nlm.nih.gov/19805638/ [PubMed: 19805638]
59. Homma T, Fujii J. Emerging connections between oxidative stress, defective proteolysis, and metabolic diseases. Free Radic Res. 2020 Apr;1–16.
60. Oparil S Comparative antihypertensive efficacy of olmesartan: comparison with other angiotensin II receptor antagonists. J Hum Hypertens [Internet]. 2002 [cited 2021 Nov 2];(2):17–23. Available from: www.nature.com/jhh

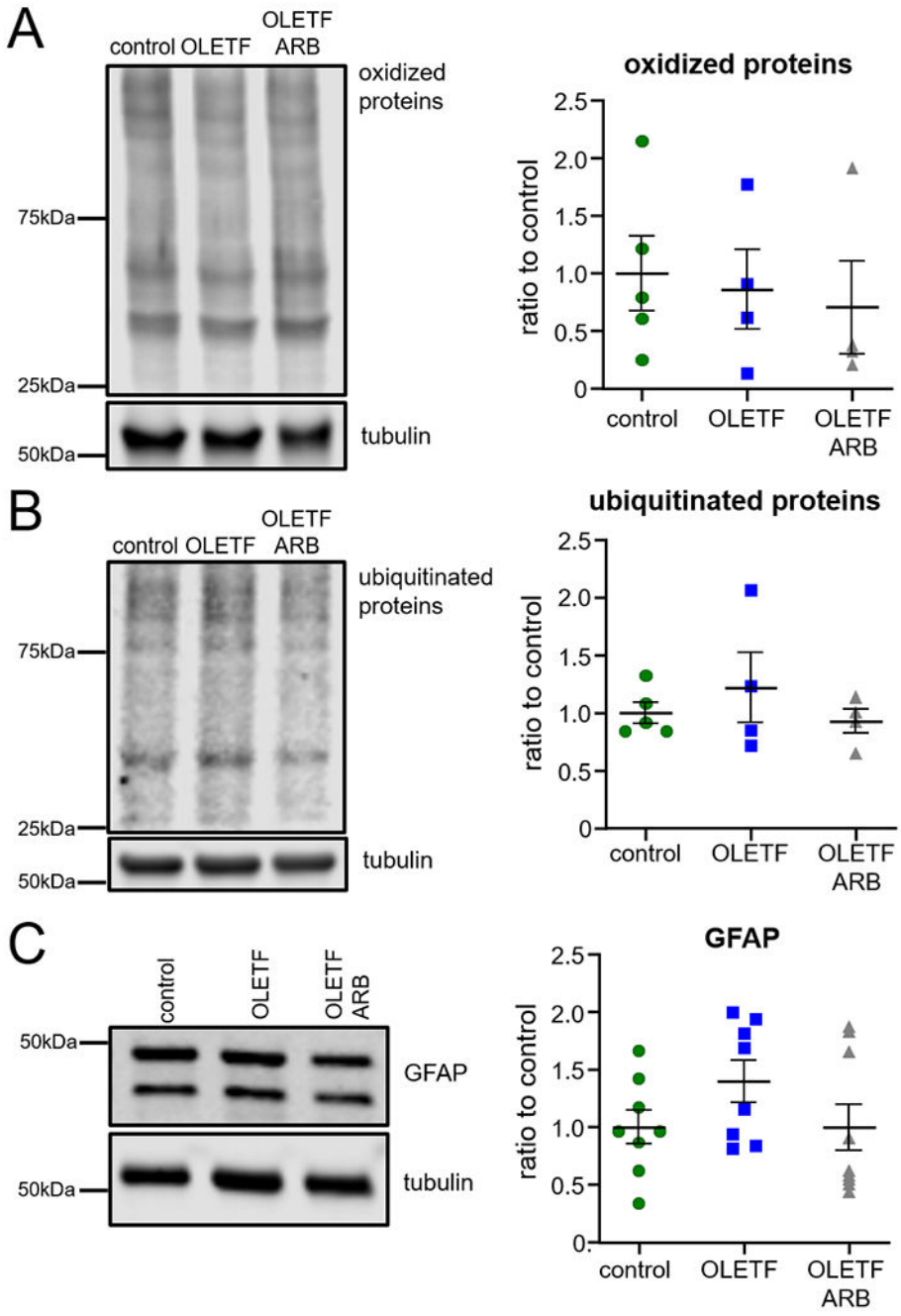


**Figure 1. Younger (16 weeks) control and OLETF animals showed similar levels of toxic protein species and the astrocyte marker, GFAP, that were not altered by ARB treatment.**

**A.** Levels of oxidized proteins by immunoblot. ANOVA $F(2,10) = 0.17$, n = 4-5. **B**. Levels of ubiquitinated proteins by immunoblot. ANOVA $F(2,10) = 0.64$, n = 4-5. **C**. Protein levels of GFAP by immunoblot. ANOVA $F(2,22) = 1.57$, n = 8-9. The housekeeping protein tubulin was used for normalization.

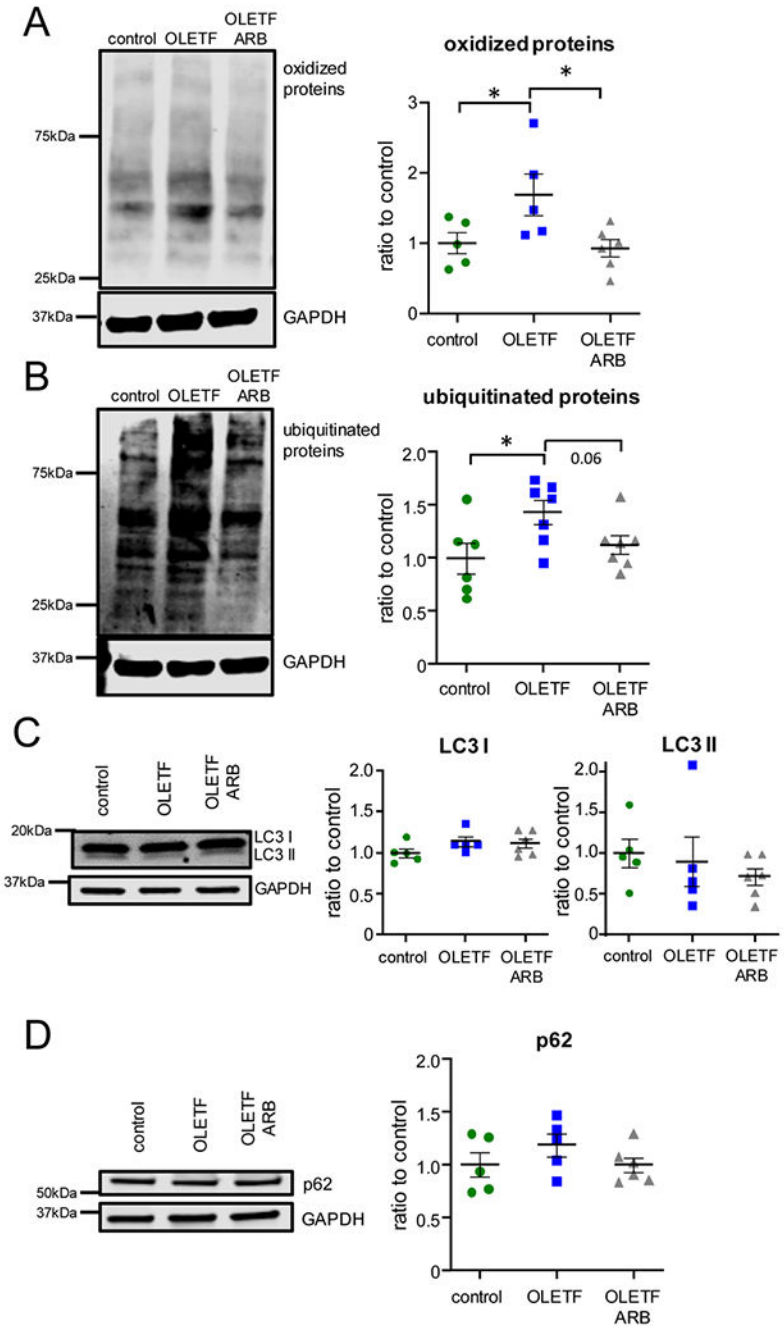


**Figure 2. Increased levels of oxidized and ubiquitinated proteins in older (25 weeks) OLETF rats were reduced by ARB.**

**A.** Levels of oxidized proteins by immunoblot. ANOVA $F(2,13) = 4.49$ $p = 0.03$, $n = 5\text{-}6$. **B**. Levels of ubiquitinated proteins by immunoblot. ANOVA $F(2,17) = 3.84$ $p = 0.04$, $n = 6\text{-}7$. **C**. Protein levels of the autophagy markers LC3-I ANOVA $F(2,13) = 1.63$ $p = 0.23$, $n = 5\text{-}6$, and LC3-II by immunoblot ANOVA $F(2,13) = 0.54$ $p = 0.59$, $n = 5\text{-}6$. **D**. Protein levels of the autophagy marker p62 by immunoblot. ANOVA $F(2,13) = 1.17$ $p = 0.34$, $n = 5\text{-}6$. The housekeeping protein GAPDH was used for normalization. * = $p \leq 0.05$.

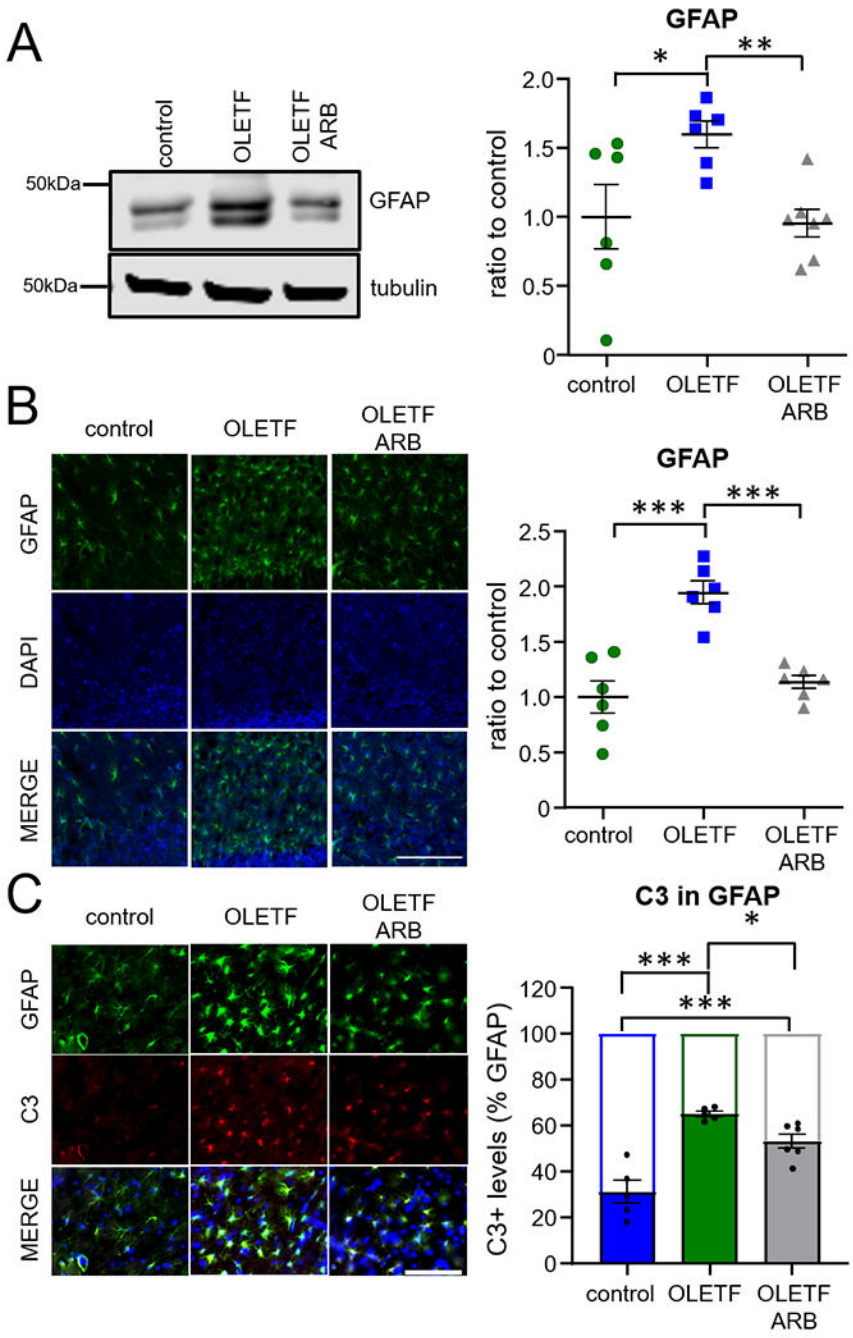


**Figure 3. Increased levels of neurotoxic astrocytes in older (25 weeks) OLETF rats were reduced by ARB.**

**A**. Protein levels of the astrocyte marker GFAP by immunoblot. ANOVA $F(2,16) = 5.53$ $p = 0.01$, $n = 6$-7. **B.** Protein levels of GFAP (green) in the hippocampus by immunofluorescent staining. ANOVA $F(2,15) = 21.92$ $p < 0.0001$, $n = 6$. Nuclear DAPI counterstaining is shown in blue. **C.** Protein levels of C3 (red) in the GFAP (green) positive population in the hippocampus by immunofluorescent staining. ANOVA $F(2,13) = 22.44$ $p < 0.0001$, $n = 5$-6.

Nuclear DAPI counterstaining is shown in blue. The open bars show the C3- population for each group. *** = $p \leq 0.001$, ** = $p \leq 0.01$, * = $p \leq 0.05$. Scale bar = 100 μm.

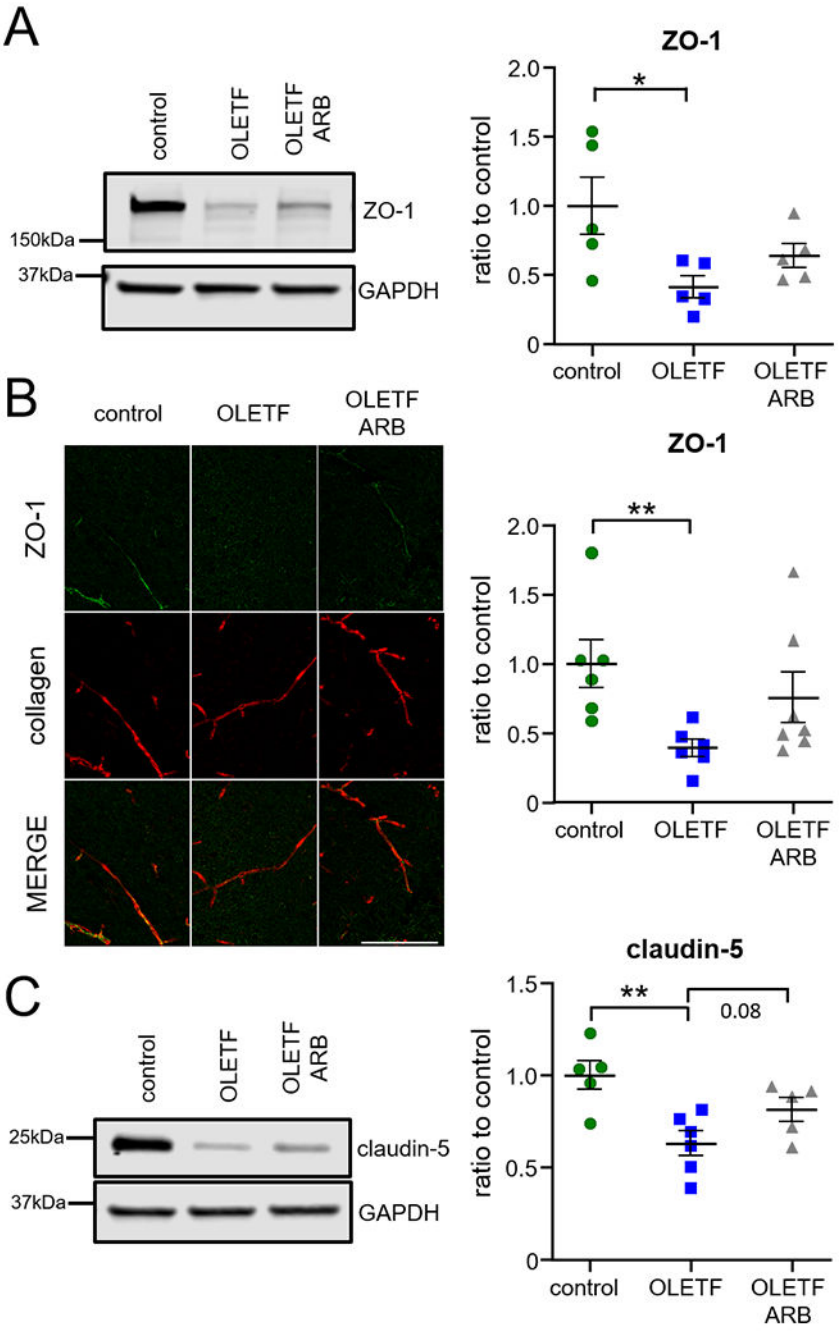


**Figure 4. Deficiencies in tight junction proteins were observed in older (25 weeks) OLETF rats.**

**A.** Protein levels of the tight junction marker ZO-1 by immunoblot. ANOVA $F(2,12) = 4.57$ $p = 0.03$, $n = 5$. **B.** Protein levels of the tight junction marker ZO-1 (green) in the hippocampus by immunofluorescent staining. Kruskal-Wallis $H(2) = 8.96$ $p = 0.005$, $n = 6\text{-}7$. Collagen staining shows vessels in red. Scale bar = 100 μm. **C.** Protein levels of the tight junction marker claudin-5 by immunoblot. ANOVA $F(2,13) = 7.2$ $p = 0.007$, $n = 5\text{-}6$ . The housekeeping protein GAPDH was used for normalization in the immunoblot experiments. ** = $p \leq 0.01$, * = $p \leq 0.05$.

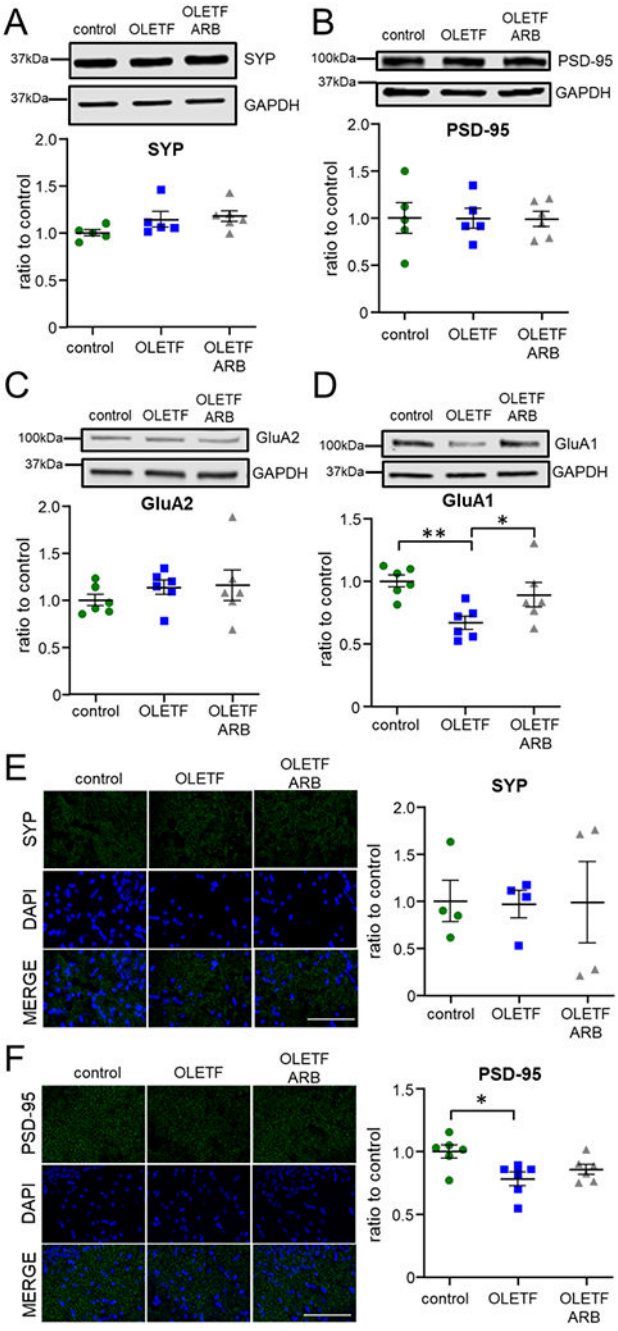


**Figure 5. Decreased levels of postsynaptic proteins were observed in older (25 weeks) OLETF rats.**

**A.** Protein levels of the presynaptic marker synaptophysin (SYP) by immunoblot. Kruskal-Wallis H(2) = 5.76, n = 5-6. **B.** Protein levels of the postsynaptic marker PSD-95 by immunoblot. ANOVA F(2,13) = 0.002, n = 5-6. **C.** Protein levels of the postsynaptic marker GluA2 by immunoblot. ANOVA F(2,15) = 0.6, n = 6. **D.** Protein levels of the postsynaptic marker GluA1 by immunoblot. ANOVA F(2,15) = 6.04 p = 0.01, n = 6. **E.** Protein levels of SYP (green) in the hippocampus by immunofluorescence. ANOVA F(2,9) = 0.003, n =

4. **F.** Protein levels of PSD-95 (green) in the hippocampus by immunofluorescence. ANOVA $F(2,15) = 5.09$ $p = 0.02$, $n = 6$. Nuclear DAPI counterstaining is shown in blue. The housekeeping protein GAPDH was used for normalization in the immunoblot experiments. ** = $p \leq 0.01$, * = $p \leq 0.05$. Scale bars = 100 μm.

**Table 1.**

List of primary antibodies used in this study

| Target | Vendor & catalog number | Application & dilution |
|---|---|---|
| GFAP | MilliporeSigma, mab360 | WB (1:1,000) |
| GFAP | Dako, Z0334 | IF (1:500 ) |
| Iba-1 | Wako, 016-20001 | WB (1:1,000 ) |
| PSD95 | Cell Signaling, 3409 | IF (1:100) |
| PSD95 | Neuromab, 73-028 | WB (1:500 ) |
| SYP | Abcam, ab14692 | WB (1:2,000 ), IF (1:100) |
| Mono- and Poly-ubiquitinated proteins (clone FK2) | Enzo lab Sciences, BML-PW8810 | WB (1:1,000) |
| ZO-1 | Invitrogen, 33-9100 | WB (1:150 ), IF (1:50) |
| claudin-5 | Invitrogen, 35-2500 | WB (1:200 ) |
| collagen IV | Invitrogen, PA1-36063 | IF (1:50) |
| tubulin | Sigma-Aldrich, B-5-1-2 | WB (1:25,000) |
| GAPDH | ProteinTech, 60004-1-Ig | WB (1:5,000) |
| C3 | Hycult Biotech, HM1045-100UG | IF (1:50) |
| LC3 | Abcam, ab48394 | WB (1:1,000 ) |
| p62 | Abcam, ab56416 | WB (1:500 ) |
| GluA2 | MilliporeSigma, MAB397 | WB (1:1,000 ) |
| GluA1 | Cell Signaling, 13185 | WB (1:1,000 ) |

WB = western blot, IF = immunofluorescence

**Table 2.**

Mean (± SE) end of study variables provided here to demonstrate basic phenotypic and metabolic changes associated with the strain and treatment of ARB (data published in different formats in [18,22,25,26]).

| | *16 Weeks of Age* | | | | *25 Weeks of Age* | | |
|---|---|---|---|---|---|---|---|
| | **LETO** | **OLETF** | **OLETF + ARB** | | **LETO** | **OLETF** | **OLETF + ARB** |
| Body Mass (g) | 425 ± 14 | 568 ± 13 * | 530 ± 6 * | | 465 ± 29 | 610 ± 31 * | 598 ± 36 * |
| [a]Relative Total Fat Mass (g/100 g BM) | 3.1 ± 0.1 | 6.3 ± 0.3 * | 6.2 ± 0.4 * | | ND † | ND † | ND |
| SBP (mm Hg) | 114 ± 5 | 139 ± 2 * | 111 ± 4 # | | 109 ± 1 | 155 ± 2 * | 113 ± 2 # |
| | | | | | | | |
| *Fasting Plasma* | | | | | | | |
| Glucose (mg/dL) | 101 ± 4 | 133 ± 4 * | 121 ± 2 *# | | 90 ± 5 | 135±23 * | 128 ± 2 * |
| Insulin (ng/mL) | 0.75 ± 0.10 | 1.71 ± 0.18 * | 1.32 ± 0.16 * | | 0.41 ± 0.06 | 0.74 ± 0.24 * | 0.62 ± 0.13 |
| Triglycerides (mg/dL) | 53 ± 9 | 124 ± 9 * | 89 ± 8 * | | 50 ± 7 | 138 ± 14 * | 107 ± 13 * |

SBP = systolic blood pressure;

[a] = “total” refers to retroperitoneal and epididymal fat masses;

ND = not determined.

† Although abdominal fat mass was not determined in 25 wk old rats, at 24 wks (similar aged) the percent abdominal fat is a 3.4% and 6.5% in LETO and OLETF, respectively -, which is consistent with the percentages determined here for 16 wk old rats. The similar body masses between OLETF and OLETF + ARB at 25 wks suggests that fat mass between the two groups was also similar.

* different from LETO at $p < 0.05$;

# different from OLETF at $p < 0.05$